Electronic Supplementary Material (ESI) for Physical Chemistry Chemical Physics.

Supplementary Information for

Mediating Both Valence and Conduction Bands of TiO_2 by Anionic Dopants for Visible- and Infrared-light Photocatalysis

Tingwei Chen, Guokui Liu, Fan Jin, Min Wei, Jin Feng and Yuchen Ma*

School of Chemistry and Chemical Engineering, Shandong University, Jinan 250100, China

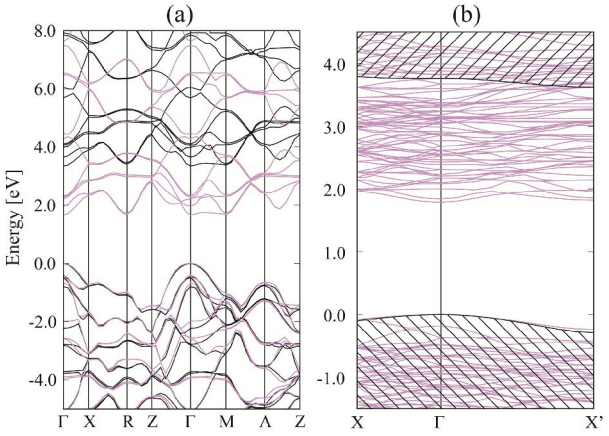

Figure S1. DFT-LDA (purple) and *GW* (black) band structures of the rutile TiO_2 bulk (a) and the three-trilayer (110) surface model with the bottom side saturated by pseudohydrogen atoms (b). For clarity, the *GW* band structure in (b) is only indicated by shaded areas. Valence band maximum is set to zero in both LDA and *GW*.

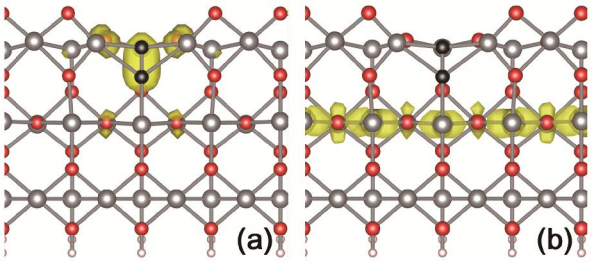

Figure S2. Spatial distribution (yellow contour) of the band-gap states for the C-doped rutile TiO_2 (110)(4×1) surface where a C_2 dimer is formed after homo-doping at sites O^0 and O^3 (see Figure 1 for details). (a) [(b)]: the lower [higher] band-gap state in the vicinity of valence [conduction] band edge. These two states are highlighted by crosses in Figure S4c. Red, grey and black balls represent O, Ti and C atoms, respectively.

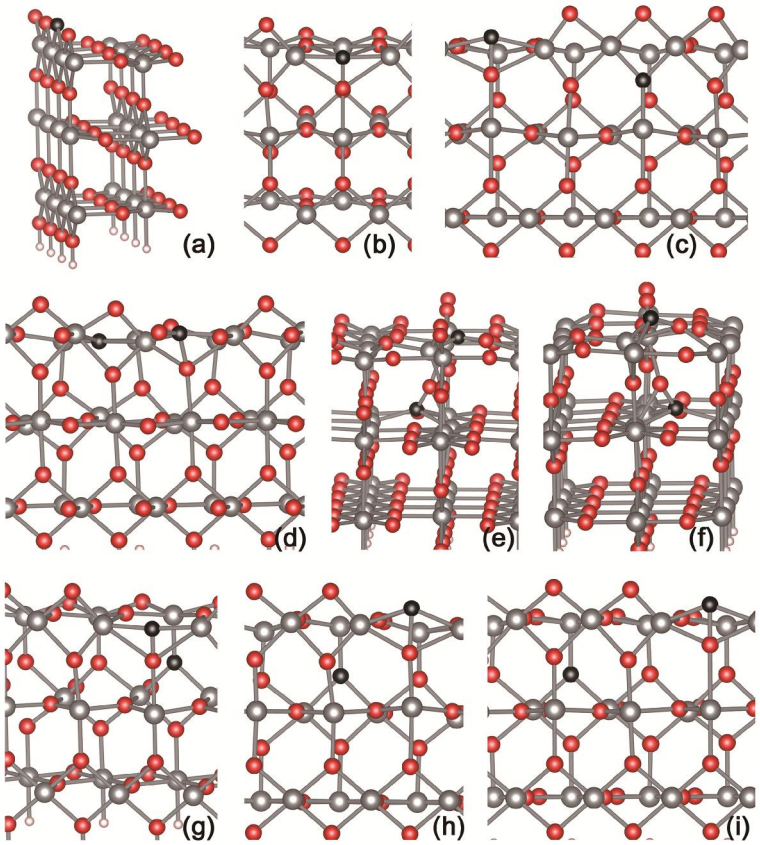

Figure S3. Some configurations for the C-doped rutile TiO_2 (110)(4×1) surface. (a) Mono-doping at site O^b without no new bond formed (case O^b(i) in Table 1). (b)-(i) Configurations with C-O bonds formed. (b) Mono-doping at site O^b (case O^b(ii) in Table 1). (c)-(i) Homo-doping at sites O^0-O^5, O^0-O^7, O^0-O^8, O^0-O^9, O^0-O^{10}, O^0-O^{11} and O^0-O^{12}, respectively (see Figure 1 for details). Red, grey and black balls represent O, Ti and C atoms, respectively.

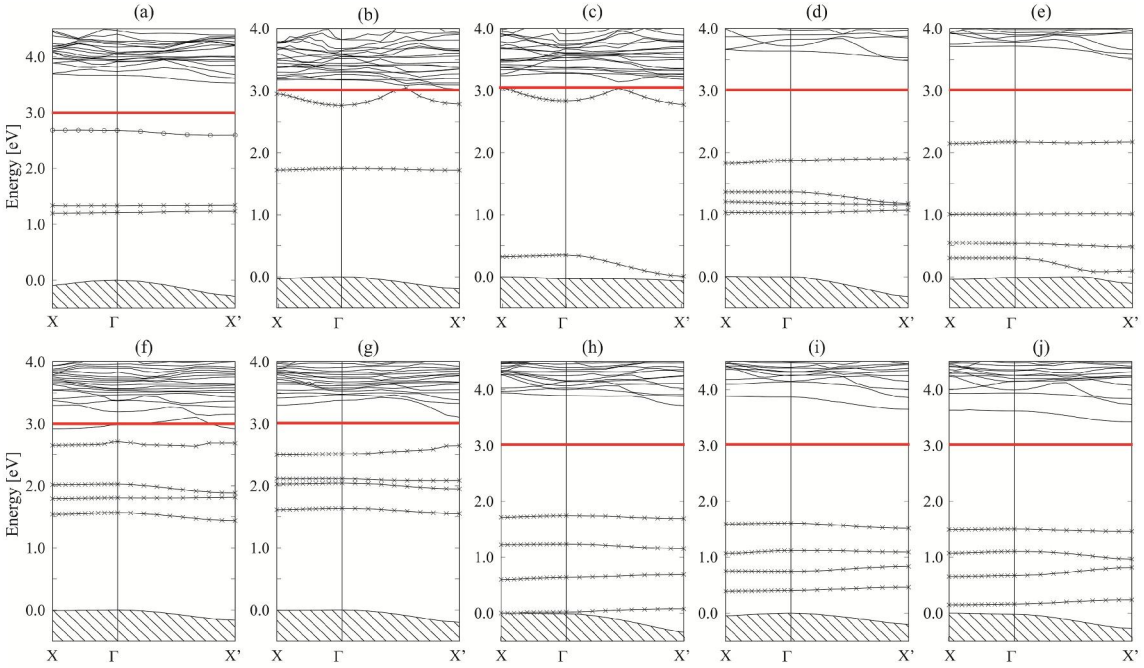

Figure S4. *GW* band structures of the C-doped rutile TiO_2 (110)(4×1) surface. (a) Mono-doping O^b(i). (b) Mono-doping O^b(ii). (c) Homo-doping O^0-O^3 where a C_2 dimer bond is formed. (d)-(j) Homo-doping O^0-O^5, O^0-O^7, O^0-O^8, O^0-O^9, O^0-O^{10}, O^0-O^{11} and O^0-O^{12}, respectively, where one or two C-O bonds are formed. Please refer to Figure S2 and Figure S3 for the configurations. Red lines indicate position of the experimental CBM which is 3.0 eV above VBM. The valence bands are represented by shaded areas.

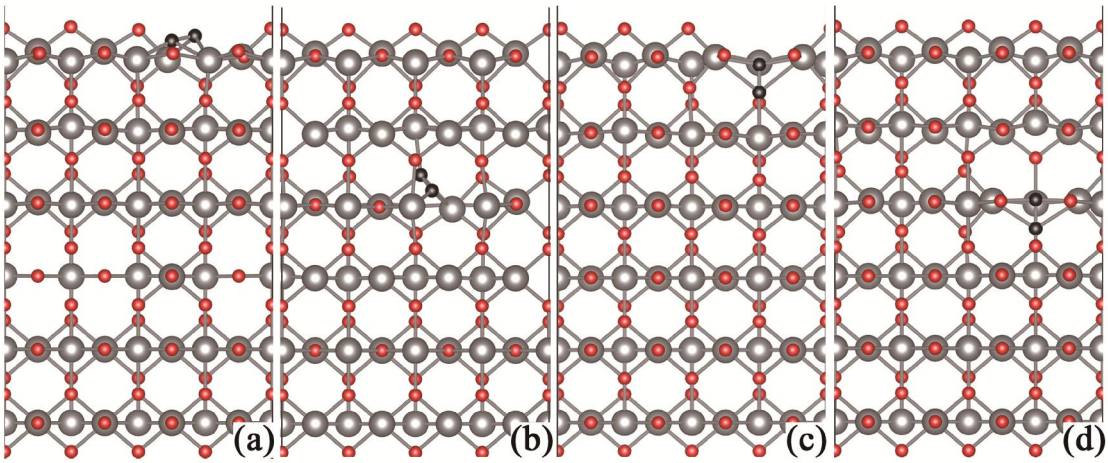

Figure S5. Configurations for homo-doping in the top surface [(a) and (c)] and the subsurface [(b) and (d)] of a six-trilayer rutile TiO_2 (110)(4×1) surface. The initial doping sites are O^0-O^6 for (a) and (b), O^0-O^3 for (c) and (d) (see Figure 1 for details). Red, grey and black balls represent O, Ti and C atoms, respectively.

Table S1. Relative total energies (in eV) of the homo-doped rutile (110) surface and subsurface by C atoms in the six-trilayer rutile TiO_2 (110)(4×1) surface model with respect to the intact surface. Columns named by C_2 list the length (in Å) of the bond of C_2 dimer.

Doping site(s)	E_{total}	C_2	Doping site(s)	E_{total}	C_2
O^0-O^6(surface)	1.69	1.27	O^0-O^3(surface)	3.14	1.24
O^0-O^6(subsurface)	3.08	1.26	O^0-O^3(subsurface)	4.19	1.28

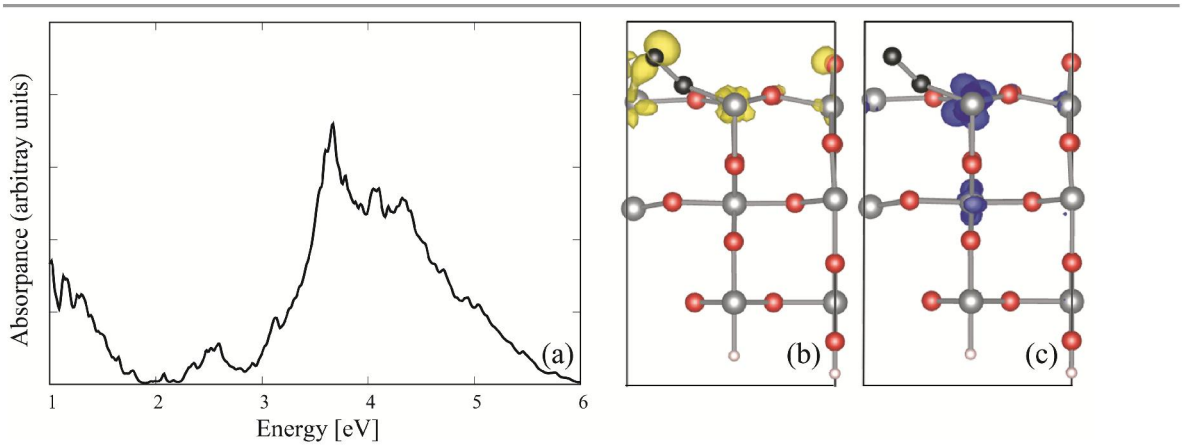

Figure S6. (a) Calculated optical absorption spectrum by BSE for the C-doped rutile TiO_2 (110)(2×1) surface where a C_2 dimer is formed after homo-doping at sites O^0 and O^6 (see Figure 1 for details). (b)-(c): Spatial distribution of the photogenerated hole (yellow isosurface) and electron (blue isosurface) for excitation at 2.08 eV which is the highest-energy transition from the filled impurity state in the vicinity of CBM (state C1 in Figure 3a). An artificial broadening of 0.02 eV is included in the BSE spectrum. Incident direction of the light is set normal to the surface in BSE.